

Antiproton Production in Au + Au Collisions at 11.7A GeV/c

L. Ahle,^{9,*} Y. Akiba,⁶ K. Ashktorab,¹ M. D. Baker,⁹ D. Beavis,¹ H. C. Britt,⁷ J. Chang,³ C. Chasman,¹ Z. Chen,^{1,†} C.-Y. Chi,⁴ Y. Y. Chu,¹ V. Cianciolo,^{9,‡} B. A. Cole,⁴ H. J. Crawford,² J. B. Cumming,¹ R. Debbe,¹ J. C. Dunlop,⁹ W. Eldredge,³ J. Engelage,² S.-Y. Fung,³ E. Garcia,⁸ S. Gushue,¹ H. Hamagaki,¹⁰ L. F. Hansen,⁷ R. S. Hayano,¹¹ G. Heintzelman,⁹ E. Judd,² J. Kang,¹³ E.-J. Kim,^{1,13} A. Kumagai,¹² K. Kurita,^{12,§} J.-H. Lee,¹ J. Luke,⁷ Y. Miake,¹² A. Mignerey,⁸ B. Moskowit,¹ M. Moulson,⁴ C. Muentz,^{1,||} S. Nagamiya,⁵ M. N. Namboodiri,⁷ C. A. Ogilvie,⁹ J. Olness,¹ L. P. Remsberg,¹ H. Sako,^{11,¶} T. C. Sangster,⁷ R. Seto,³ J. Shea,⁸ K. Shigaki,^{11,**} R. Soltz,^{9,‡} S. G. Steadman,⁹ G. S. F. Stephans,⁹ M. J. Tannenbaum,¹ J. H. Thomas,^{7,††} S. Ueno-Hayashi,¹² F. Videbaek,¹ F. Wang,^{4,‡‡} Y. Wu,⁴ H. Xiang,³ G. H. Xu,³ K. Yagi,¹² H. Yao,⁹ W. A. Zajc,⁴ and F. Zhu¹
(E-802 Collaboration)

¹Brookhaven National Laboratory, Upton, New York 11973

²Space Sciences Laboratory, University of California, Berkeley, California 94720

³University of California, Riverside, California 92507

⁴Columbia University, New York 10027

and Nevis Laboratories, Irvington, New York 10533

⁵High Energy Accelerator Research Organization (KEK), Tsukuba, Ibaraki 305, Japan

⁶High Energy Accelerator Research Organization (KEK), Tanashi-branch, (Tanashi) Tokyo 188, Japan

⁷Lawrence Livermore National Laboratory, Livermore, California 94550

⁸University of Maryland, College Park, Maryland 20742

⁹Massachusetts Institute of Technology, Cambridge, Massachusetts 02139

¹⁰Center for Nuclear Study, School of Science, University of Tokyo, Tanashi, Tokyo 188, Japan

¹¹Department of Physics, University of Tokyo, Tokyo 113, Japan

¹²University of Tsukuba, Tsukuba, Ibaraki 305, Japan

¹³Yonsei University, Seoul 120-749, Korea

(Received 7 May 1998)

Antiproton production in 11.7A GeV/c Au + Au collisions over a wide transverse-mass coverage was studied using the AGS-E866 experimental apparatus. The mean transverse kinetic energy increases as a function of centrality and is similar to that of protons. The antiproton yields in Si + Al, Si + Au, and Au + Au collisions are consistent with scaling with the 0.7 power of the number of participant nucleons. [S0031-9007(98)07191-9]

PACS numbers: 25.75.Dw, 13.85.Ni, 21.65.+f

Antiproton (\bar{p}) yields in relativistic heavy ion collisions reflect a subtle competition between initial production in nucleon-nucleon collisions and subsequent annihilation on the surrounding nucleons. At AGS energies \bar{p} production in N + N collisions is near the threshold and is quite small. However, several processes in heavy ion reactions are expected to increase the yield. An anomalously high \bar{p} yield has been proposed as an indication of the quark-gluon-plasma [1,2] and chiral restoration [3]. Less exotic hadronic multistep processes have also been considered for enhancing \bar{p} production in the cascade code RQMD [4,5]. In contrast, the large \bar{p} annihilation cross section is expected to reduce the final yield. For these reasons the \bar{p} yield has been suggested as a measure of the high baryon density [6,7] predicted as about 10 times the normal nuclear density in Au + Au collisions at AGS energies by cascade models RQMD [7], ARC [8], and ART [9]. By measuring \bar{p} yields systematically, it may be possible to disentangle the effects of production and absorption. This paper presents differential \bar{p} yields as a function of centrality

for Au + Au reactions and compares the results to those for $p + A$ and $Si + A$ reactions.

Three representative pictures have been proposed for \bar{p} production at AGS energies. The most naive model uses a superposition of each collision between an unstruck projectile and an unstruck target nucleon with no subsequent absorption. This "first collision model" [10] provides a base line for the initial production especially near threshold. The sophisticated cascade models, ARC and RQMD, implement two complementary approaches to \bar{p} yields. ARC [11] allows production on every sequential NN collision through energy dependent cross sections. Absorption is greatly reduced through a three-body screening mechanism. RQMD [12], on the other hand, combines the large enhancement of initial production from hadronic multistep processes with strong absorption through free \bar{p} absorption cross sections. In short, the three scenarios are first hit production with no absorption, normal production with screened absorption, and enhanced production and strong absorption. In previous measurements at the AGS, \bar{p} yields in $p + A$ and $Si + A$ collisions are consistent

with scaling with the number of projectile participant nucleons [13] as expected in the first collision model.

The E866 experiment was built to study particle production in Au + Au collisions over a wide rapidity y and transverse mass $m_t = \sqrt{m_p^2 + p_t^2}$, where m_p is the \bar{p} mass, and p_t is the transverse momentum. The experimental setup is described elsewhere [14,15]. The analysis presented here uses data taken with the forward magnetic spectrometer in 1994 using a ^{197}Au beam at $11.67 \pm 0.03A$ GeV/ c and an Au target of 975 mg/cm 2 (about 2% beam interaction rate). It covers polar angles from 6° to 24° and its kinematic coverage for \bar{p} is $1.0 < y < 2.2$ and $0 < m_t - m_p < 1.2$ [GeV/ c^2]. The nucleon-nucleon center-of-mass (c.m.) rapidity y_{NN} is at 1.6. Particle identification (PID) is made with a 100-slat time-of-flight detector (FTOF) with 75 ps rms resolution placed 6 m from the target. Momentum resolution for \bar{p} was estimated to be $\sigma_p/p = 1.5\%$ at $p = 0.5$ GeV/ c and 5% at $p = 5$ GeV/ c . A zero-degree calorimeter (ZCAL) was used to define the centrality of the collision by measuring the total kinetic energy E_{ZCAL} of projectile spectators. A zero-degree Čerenkov detector measured the charge of the forward-going particles and provided an interaction trigger (INT). The data were taken with a spectrometer trigger (FSPEC) that required INT and hits on drift chamber planes. The FSPEC efficiency was better than 99.9%. Data were also taken with the Henry Higgins E802 spectrometer [16]. These data serve as independent confirmation of the experimental consistency.

The track reconstruction procedure is described elsewhere [15]. To suppress backgrounds due to multiple hits in an FTOF slat, a cut is applied to the energy deposited in the slat. A PID cut was applied in the m^2 vs p plane, where $m^2 = p^2[(\frac{ct}{l})^2 - 1]$, with the velocity of light c , the time-of-flight t , and the track path length l . The cut boundary was set at $\pm 2.5\sigma$ from m_p^2 in $p < 3$ GeV/ c , and was extended to $p = 4.5$ GeV/ c by excluding the region with a high contamination of π^- and K^- . The background level was kept to 10%–20%. The number of \bar{p} candidates was about 800 out of 15 million FSPEC events.

Invariant cross sections ($Ed^3\sigma/dp^3$) were obtained in minimum bias events, and with centrality cuts. Correction factors were applied to every identified \bar{p} . Typical values of these factors for the most central 10% events are given by: track reconstruction (~ 1.07), FTOF multiple hits in a slat (~ 1.10), hadronic absorption in the target and detectors (~ 1.02), FTOF energy loss cut (~ 1.11), and background subtraction (~ 0.85). The total systematic error was evaluated to be about 10%. The centrality is defined as the trigger cross section integrated from zero to the measured E_{ZCAL} , normalized to the total interaction cross section of 6.85 b [17]. Four centrality windows are used in this analysis; 0%–8%, 8%–23%, 23%–38%, and 38%–77%, where 0% corresponds to the most central event, and 77% corresponds to the INT cross section of 5.3 b. A fraction of the inclusive \bar{p} yield lost by the INT

trigger bias is estimated to be only about 8%, and not corrected for.

Figure 1 shows \bar{p} yields $Ed^3N/dp^3 \equiv (1/\sigma_{\text{trig}}) \times Ed^3\sigma/dp^3$, in minimum bias events, where σ_{trig} denotes the trigger cross section. Spectra at symmetric rapidities with respect to $y_{NN} = 1.6$ are consistent within errors. Figure 2 shows \bar{p} invariant differential yields in the four centrality windows. Each \bar{p} spectrum in Fig. 2 is fitted to a single exponential form with the rapidity density (dN/dy) and the inverse slope parameter (T)

$$\frac{d^2\sigma}{2\pi\sigma_{\text{trig}}m_t dm_t dy} = \frac{dN/dy}{2\pi T(T + m_p)} \exp\left(-\frac{m_t - m_p}{T}\right). \quad (1)$$

Table I shows dN/dy and $\langle m_t - m_p \rangle$ for the different centrality cuts and for comparison also shows these values for protons (p). The inverse slope parameter, T , and $\langle m_t - m_p \rangle$ demonstrate that the \bar{p} spectra become flatter with increasing centrality. It is also evident that the $\langle m_t - m_p \rangle$ increases with centrality similarly for both protons and antiprotons.

It is known that the p spectra have a pronounced flattening at low m_t [15] and cannot be fitted satisfactorily with the single exponential form of Eq. (1) except for the most peripheral centrality cut. It is certainly of

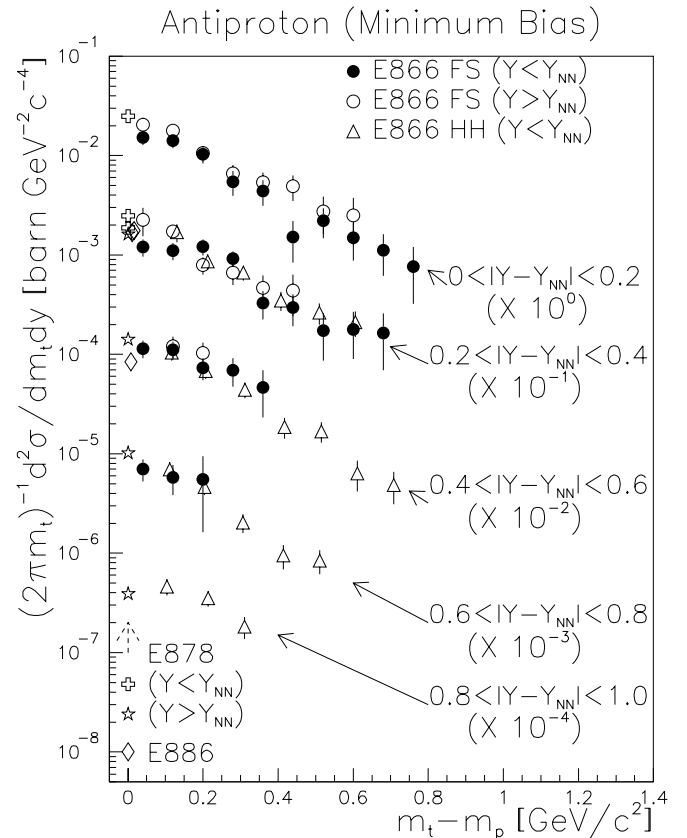


FIG. 1. Invariant differential cross sections of \bar{p} as a function of $m_t - m_p$ for minimum-bias events at each rapidity range. Data from other AGS experiments are also shown. Error bars are statistical. See text for details.

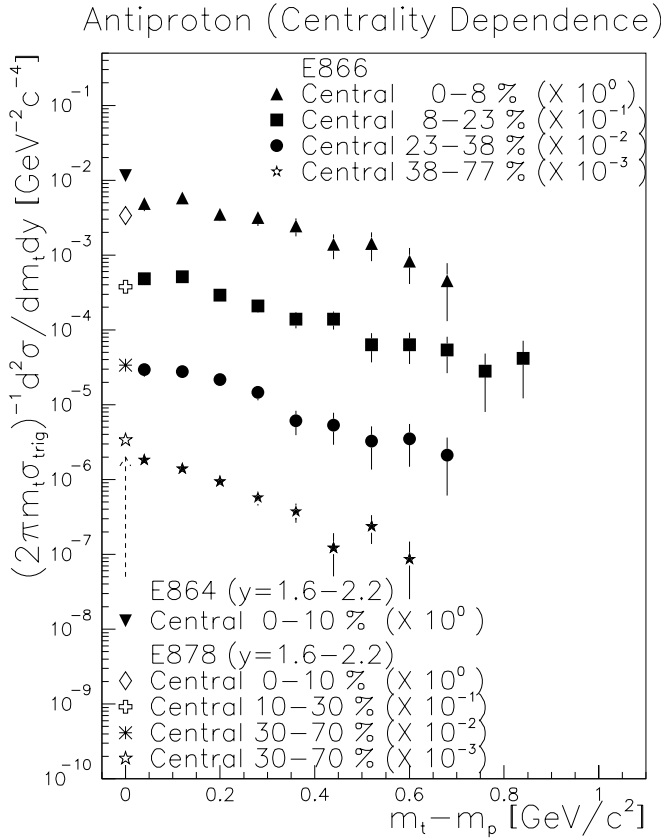


FIG. 2. Invariant differential yields of \bar{p} in $1.0 < y < 2.2$ in four centrality windows, 0%–8%, 8%–23%, 23%–38%, and 38%–77%, from top to bottom. Data from other AGS experiments are also shown. Error bars are statistical. See text for details.

considerable interest to know whether the \bar{p} spectra have the same shape. For this purpose the data were also fitted with a form proportional to the double exponential used for the p spectra [15]. The χ^2/dof of both fits is comparable and less than 1 for all centrality windows, indicating that it is statistically hard to distinguish which shape describes the \bar{p} data better.

Three other AGS experiments measured \bar{p} at $p_t \approx 0$ in Au + A collisions [18–20]. Their data are also plotted in the figures. E878 data (at 10.8A GeV/c) have been scaled to 11.7A GeV/c by applying a beam energy correction factor of 1.4 explained below. For inclusive and peripheral events, data among the experiments are consistent. However, for the most central events, E864 data is a factor of 4 larger than E878 data, and the present

results lie between them by using a single exponential extrapolation. It has been suggested that the large spread among the experiments is due to differences in the acceptances for \bar{p} from $\bar{\Lambda}$ decay [20]. The acceptance including the branching ratio for \bar{p} from $\bar{\Lambda}$ decay in this experiment has been estimated as 40% by a Monte Carlo method using spectral shapes from RQMD 2.1. Since RQMD gives the ratio, $\bar{\Lambda}/\bar{p}$, for direct production as about 40%, the final anti-Lambda contribution to these results is about 14%. No correction is applied to the data presented here.

The \bar{p} yields in this experiment are compared with those in $p + A$ and $\text{Si} + A$ at 14.6A GeV/c. In order to compare different collision systems and centralities, N_{part} , the number of target and projectile nucleons that have interacted, is used. In this analysis, FRITIOF 1.7 [21] is used to estimate N_{part} from the measured cross section of each centrality window. Alternatively, for symmetric $A + A$ collisions, N_{part} is directly estimated from E_{ZCAL} and beam energy E_{BEAM} as $N_{\text{part}}^{\text{ZCAL}} = 2A(1 - E_{\text{ZCAL}}/E_{\text{BEAM}})$, where the factor of 2 comes from the symmetry of the collision system. The difference between N_{part} with FRITIOF and $N_{\text{part}}^{\text{ZCAL}}$ in Au + Au is 4% for the most central window and 35% for the most peripheral window, which is regarded as systematic uncertainty in N_{part} .

Since $p + A$ and $\text{Si} + A$ data and Au + Au data are taken at different beam energies, a correction has been applied. As a base line approximation the correction factor is determined by a \bar{p} production cross section in $p + p$ collisions at the initial beam energy. The following parametrization is used as proposed in Refs. [22,23]:

$$\sigma_{pp \rightarrow \bar{p}}(\sqrt{s}) = a(\sqrt{s} - 4m_p)^b \text{ [mb]}, \quad (2)$$

where \sqrt{s} is the total c.m. energy in GeV and a and b are fit parameters. A fit to the data from Refs. [24,25] yields $a = (1.06 \pm 0.04) \times 10^{-2}$, $b = 1.95 \pm 0.19$. Thus the energy correction necessary to compare Au + Au data at 11.7A GeV/c with $p + A$ or $\text{Si} + A$ data at 14.6A GeV/c was calculated to be 0.47 ± 0.03 , where the error is statistical. The correction factor was checked for \bar{p} data in $p + \text{Be}$ collisions at 12.9 GeV/c [26], at 14.6 GeV/c [13], and at 23.1 GeV/c [27]. Another systematic effect comes in comparing yields in limited rapidity ranges. In each collision system, dN/dy is compared in $y_{NN} - 0.6 < y < y_{NN}$, or $|y - y_{NN}| < 0.6$

TABLE I. dN/dy , T , and $\langle m_t - m_p \rangle$ for \bar{p} , and dN/dy and $\langle m_t - m_p \rangle$ for p in four centrality windows in $1.0 < y < 2.2$. The errors are statistical.

Centrality	$dN_{\bar{p}}/dy$ ($\times 10^3$)	$T_{\bar{p}}$ [MeV/c ²]	$\langle m_t - m_p \rangle_{\bar{p}}$ [MeV/c ²]	dN_p/dy	$\langle m_t - m_p \rangle_p$ [MeV/c ²]
0%–8%	15.4 ± 1.5	275 ± 31	337 ± 43	61.7 ± 0.6	328 ± 4
8%–23%	12.4 ± 0.9	251 ± 25	304 ± 34	39.9 ± 0.4	307 ± 3
23%–38%	6.97 ± 0.63	224 ± 25	267 ± 34	22.6 ± 0.2	280 ± 2
38%–77%	3.22 ± 0.24	179 ± 16	208 ± 21	5.82 ± 0.06	238 ± 3

in Au + Au. The width of dN/dy , σ_y , ranges from 0.4 for $p + \text{Be}$ collisions to 0.6 for central 0%–10% Au + Au collisions [19,26,28]. No correction for the widths has been made. Systematic change of dN/dy due to the variation in σ_y is about 20%.

Figure 3 shows dN/dy of \bar{p} 's for $p + A$ [13], Si + A [10], and Au + Au collisions as a function of N_{part} . The rapidity ranges are $1.1 < y < 1.7$ for $p + A$ and Si + A ($y_{NN} = 1.7$), and $1.0 < y < 2.2$ for Au + Au. The beam energy correction of 0.47 is applied for $p + A$ and Si + A collisions. For $p + A$, dN/dy in this rapidity range is converted from dN/dy data in $1.0 < y < 1.6$, assuming a Gaussian distribution with $\langle y \rangle = 1.7$ and $\sigma_y = 0.4$. The systematic error due to this assumption was estimated to be about 30% by changing $\langle y \rangle$ from 1.2 to 1.7. The horizontal error bars show systematic uncertainties of N_{part} described above. The dotted line shows a fit with $dN/dy = \alpha N_{\text{part}}^\beta$, where $\alpha = (2.1 \pm 1.2) \times 10^{-4}$ and $\beta = 0.74 \pm 0.12$ are obtained. If Si + A data and Au + Au data are fitted separately, β is 0.60 ± 0.24 and 0.80 ± 0.13 , respectively.

The solid and dashed curves show RQMD [29] and the first collision model calculations, respectively. RQMD

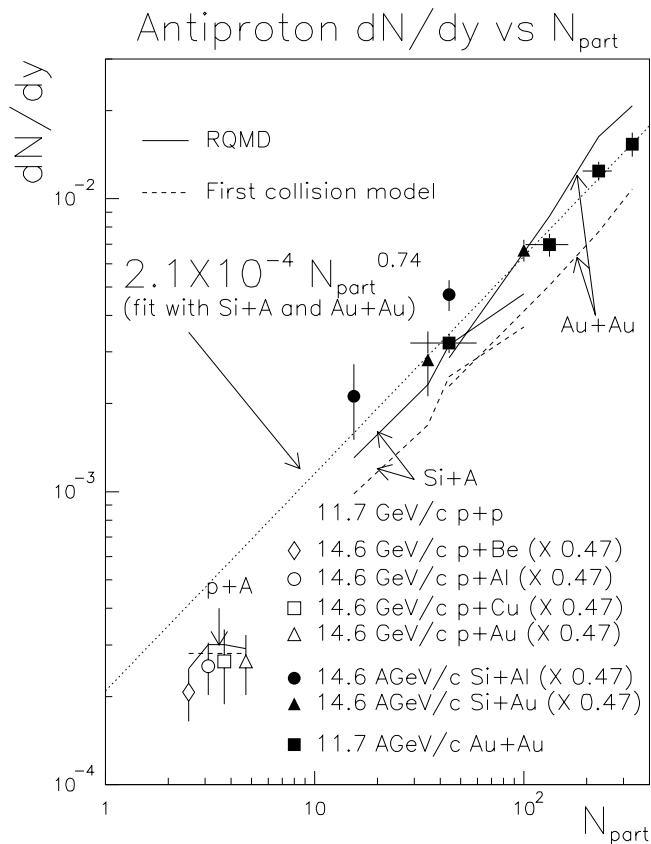


FIG. 3. dN/dy of \bar{p} in $p + A$, Si + A, and Au + Au collisions as a function of N_{part} (symbols). The dotted line shows the fit with $\alpha N_{\text{part}}^\beta$ in Si + A and Au + Au collisions. RQMD and the first collision model calculations are shown as solid and dashed curves, respectively. Vertical error bars are statistical. See text for details.

calculations are from Ref. [12] for $p + A$ and were done for Si + A and Au + Au with version 2.3. Since $p + A$ and Si + A calculations were done at 14.6 GeV/c, the same beam energy correction of 0.47 is applied. The first collision model gives \bar{p} yields as $dN/dy = dN/dy_{p+p} N_f$, where dN/dy_{p+p} is dN/dy in $p + p$ collisions which is calculated as 6.0×10^{-4} from Eq. (2). The number of first collisions, N_f is estimated with FRITIOF 1.7.

For $p + A$ collisions, both models are consistent with the experimental data. For Si + A and Au + Au collisions, both models describe the scaling with N_{part} well with RQMD rising somewhat more rapidly than the measurements. RQMD, however, gives better absolute values for the yields with the naive first collision model underestimating the cross section by 30%–50%.

In summary, \bar{p} invariant cross sections have been measured in 11.7A GeV/c Au + Au collisions as a function of the centrality of the collision. The mean transverse kinematic energy increases as a function of centrality and is similar to that of p in all centrality windows. The midrapidity \bar{p} yields in Si + Al, Si + Au, and Au + Au collisions scale as N_{part}^β with $\beta = 0.74 \pm 0.12$. RQMD predicts the dependence with N_{part} reasonably well and much of the $\langle m_t - m_p \rangle$ increases with centrality. Although entirely different conceptually, the naive first collision model also predicts the dependence of N_{part} , but, of course, cannot reproduce the strong variation in $\langle m_t - m_p \rangle$. Improved systematic measurements will be necessary to distinguish between the different models more definitely, to better estimate the nuclear density achieved, and to determine whether the shapes of the p and \bar{p} spectra are indeed similar.

This work is supported by the U.S. Department of Energy under contracts with BNL (No. DE-AC02-98CH10886), Columbia University (No. DE-FG02-86-ER40281), LLNL (No. W-7045-ENG-48), MIT (No. DE-AC02-76ER03069), UC Riverside (No. DE-FG03-86ER40271), by NASA (No. NGR-05-003-513) under contract with University of California, by Ministry of Education and KOSEF (No. 951-0202-032-2) in Korea, and by the Ministry of Education, Science, Sports, and Culture of Japan.

*Present address: Lawrence Livermore National Laboratory, Livermore, CA 94550.

†Present address: Renaissance Technologies Corp., Stony Brook, NY 11790.

‡Present address: Oak Ridge National Laboratory, Oak Ridge, TN 37831.

§Present address: The Institute of Physical and Chemical Research (RIKEN), Saitama 351-01, Japan.

||Present address: Goethe Universitaet, Institut fuer Kernphysik, Frankfurt, Germany.

¶Present address: University of Tsukuba, Tsukuba, Ibaraki 305, Japan.

- **Present address: Center for Nuclear Study, School of Science, University of Tokyo, Tanashi, Tokyo 188, Japan.
- ††Present address: Lawrence Berkeley National Laboratory, Berkeley, CA 94720.
- [1] K. S. Lee *et al.*, Phys. Rev. C **37**, 1452 (1988); D. H. Rischke *et al.*, Phys. Rev. D **41**, 111 (1990); C. M. Ko *et al.*, Phys. Rev. C **38**, 179 (1988); T. DeGrand, Phys. Rev. D **30**, 2001 (1984).
- [2] U. Heinz *et al.*, Z. Phys. A **318**, 247 (1984); U. Heinz *et al.*, J. Phys. G **12**, 1237 (1986).
- [3] J. Ellis *et al.*, Phys. Lett. B **233**, 233 (1989).
- [4] A. Jahns *et al.*, Z. Phys. A **341**, 243 (1992).
- [5] A. Jahns *et al.*, Phys. Rev. Lett. **68**, 2895 (1992).
- [6] S. Gavin *et al.*, Phys. Lett. B **234**, 175 (1990).
- [7] H. Sorge *et al.*, Phys. Lett. B **243**, 7 (1990).
- [8] Y. Pang *et al.*, Phys. Rev. Lett. **68**, 2743 (1992).
- [9] B. A. Li and C. M. Ko, Phys. Rev. C **52**, 2037 (1995).
- [10] E802 Collaboration, T. Abbott *et al.*, Phys. Lett. B **271**, 447 (1991).
- [11] S. H. Kahana *et al.*, Phys. Rev. C **47**, R1356 (1993); S. H. Kahana *et al.*, Phys. Rev. Lett. **78**, 3418 (1997).
- [12] A. Jahns *et al.*, Phys. Lett. B **308**, 11 (1993).
- [13] E802 Collaboration, T. Abbott *et al.*, Phys. Rev. C **47**, R1351 (1993).
- [14] L. Ahle *et al.*, Nucl. Phys. **A610**, 139c (1996).
- [15] L. Ahle *et al.*, Phys. Rev. C **57**, R466 (1998).
- [16] T. Abbott *et al.*, Nucl. Instrum. Methods Phys. Res., Sect. A **290**, 41 (1990).
- [17] T. F. Hoang *et al.*, Z. Phys. C **29**, 611 (1985).
- [18] E886 Collaboration, G. E. Diebold *et al.*, Phys. Rev. C **48**, 2984 (1993).
- [19] E878 Collaboration, D. Beavis *et al.*, Phys. Rev. Lett. **75**, 3633 (1995); E878 Collaboration, D. Beavis *et al.*, Phys. Rev. C **56**, 1521 (1997).
- [20] E864 Collaboration, T. A. Armstrong *et al.*, Phys. Rev. Lett. **79**, 3351 (1997).
- [21] B. Nilsson-Almqvist *et al.*, Comput. Phys. Commun. **43**, 387 (1987).
- [22] G. Q. Li *et al.*, Phys. Rev. C **49**, 1139 (1994).
- [23] G. Batko *et al.*, Phys. Lett. B **256**, 331 (1991).
- [24] C. S. Shen *et al.*, Phys. Rev. **171**, 1344 (1968).
- [25] T. K. Gaisser *et al.*, Phys. Rev. D **11**, 3157 (1975).
- [26] A. Yamamoto, Ph.D. thesis, University of Tokyo, 1981 (unpublished).
- [27] D. Dekkers *et al.*, Phys. Rev. **137**, B962 (1965).
- [28] E858 Collaboration, P. Stankus *et al.*, Nucl. Phys. **A554**, 603c (1992).
- [29] H. Sorge *et al.*, Nucl. Phys. **A498**, 567c (1989).